Calculated electron impact spin-coupled rotational cross-sections for $^{2S+1}\Sigma^{+}$ linear molecules: CN as an example

2012 J. Phys. B: At. Mol. Opt. Phys. 45 175202

(http://iopscience.iop.org/0953-4075/45/17/175202)

J. Phys. B: At. Mol. Opt. Phys. **45** (2012) 175202 (8pp) doi:10.1088/0953-4075/45/17/175202

Calculated electron impact spin-coupled rotational cross-sections for $^{2S+1}\Sigma^+$ linear molecules: CN as an example

Stephen Harrison[1], **Jonathan Tennyson**[1] **and Alexandre Faure**[2]

[1] Department of Physics and Astronomy, University College London, Gower Street, London WC1E 6BT, UK
[2] UJF-Grenoble 1/CNRS-INSU, Institut de Planétologie et d'Astrophysique de Grenoble (IPAG) UMR 5274, Grenoble F-38041, France

E-mail: j.tennyson@ucl.ac.uk

Received 2 June 2012, in final form 17 July 2012
Published 9 August 2012
Online at stacks.iop.org/JPhysB/45/175202

Abstract
Here we present the development and adaptation of existing atom–molecule collision theory in order to calculate spin-coupled rotationally resolved cross-sections for electron–molecule collisions. A full theory is developed from the existing work for this new process and then implemented using the infinite order sudden approximation to simplify the method; this approximation is shown to hold for the results of a simple test. The formalism is used to compute spin-rotation cross-sections for electron collisions with the CN radical in its $^2\Sigma^+$ ground electronic state. Results for transitions out of the ground spin rotational state are presented. A general fortran program, ROTLIN_S, is developed for this task.

(Some figures may appear in colour only in the online journal)

1. Introduction

Electron collisions provide a route to excitation in even weakly ionized plasmas. While most plasmas are not studied at rotational resolution, this is not true of the cold astronomical plasmas in the interstellar medium (ISM), that form both dense and diffuse molecular clouds. Electron–molecule collisions are important in other astronomical environments including planetary nebulae, cometary tails and planetary aurora. Thus, for example, rotational emission spectra have been used to provide the most direct estimate available of the electron density in a shocked region of the ISM (Jimenez-Serra *et al* 2006) and hence to study differences in the behaviour of ionized and neutral molecules (Roberts *et al* 2010).

Given that none of the environments mentioned above are in local thermodynamic equilibrium, electron collision cross-sections are required to model any observed emission due to electron impact excitation. The laboratory measurement of electron impact rotational excitation cross-section is extremely challenging and very few such measurements are available. This has placed the onus on theory to provide the necessary data.

R-matrix calculations, combined with a Coulomb–Born treatment for high electron angular momenta, were originally developed for the treatment of electron collisions with linear molecular ions (Rabadán *et al* 1998a, 1998b, Rabadán and Tennyson 1998, Lim *et al* 1999, Faure and Tennyson 2001). Comparison of calculations performed for several species showed that while for systems with dipoles larger than about 2 Debye, excitations with $\Delta J = 1$ are both completely dominant and well-treated by the Coulomb–Born formula of Chu and Dalgarno (1974), transitions with $\Delta J \neq 1$ are important for less polar molecules and such systems require the detailed treatment of short-range interactions provided by the *R*-matrix methodology.

The work on linear ions was subsequently extended to nonlinear ions (Faure and Tennyson 2002a, 2002b) and neutral molecules (Faure *et al* 2004). Electron impact rotational excitation with a number of closed-shell linear molecules has been considered including HCN and HNC (Faure *et al* 2007), SiO (Varambhia *et al* 2009) and CS (Varambhia *et al* 2010). For the HCN system, Faure *et al* (2007) extended the theoretical treatment to allow for hyperfine effects. The data on electron impact rotational excitation of neutral and ionized molecules

of astrophysical interest is gathered in the BASECOL database (Dubernet *et al* 2012).

The difficulty of measuring rotational excitation cross-sections makes it hard to assess independently the reliability of the cross-sections mentioned above. However evidence from experimental studies on cooling of HD^+ by electrons (Shafir *et al* 2009) and electron collisions with water (Faure *et al* 2004, Itikawa and Mason 2005, Zhang *et al* 2009), as well as comparison with detailed close-coupling calculations (Faure *et al* 2006), all point towards the reliability of this procedure.

So far all the studies considered above have only treated closed shell systems. Open shell species introduce new sources of angular momentum in the collision system and therefore require a generalization of the methodological developments described above. In this work we re-formulate the theory of electron impact rotational excitation for the case of a linear molecule with total electron spin angular momentum, S, greater than zero. In this we follow the work of Corey and McCourt (1983), who considered collisions between a $^{2S+1}\Sigma^+$ linear molecule and an atom in a ^{1}S state. As an electron has $s = 1/2$, it is necessary to consider an extra spin in our treatment. Currently we know of no other computation implementations for calculating spin-coupled rotational cross-sections driven by electron impact, however there has been recent work published on spin-inclusive rovibrational cross-sections for atom–molecule systems (Lopez-Duran *et al* 2008). Similarities exist with this work in that the atom in question is treated as structureless, which is also the initial assumption for the projectile used here.

As an example we consider electron collision cross-sections for the cyanogen molecule, CN, which has a $^2\Sigma^+$ symmetry electronic ground state. CN was one of the earliest molecules detected in the ISM and it has been observed in a variety of different astronomical environments (Bus *et al* 1991, Ahearn *et al* 1995, Fray *et al* 2005, Giannetti *et al* 2012). The CN rotational spectrum has been used to measure the temperature of the cosmic microwave background along different lines of sight. However whether the collisional excitation by species including electrons contribute to an enhanced observed temperature for the rotational states of CN has proved controversial (Roth *et al* 1993, Leach 2012). Electron collisional excitation of CN was considered sometime ago by Crawford *et al* (1969) and Allison and Dalgarno (1971), and recently by Harrison and Tennyson (2012).

This paper is divided as follows. The next section presents a general theory for calculating spin resolved electron impact rotational excitation cross-sections. Use of the infinite order sudden (IOS) approximation is discussed in section 3. Section 4 tests the IOS approximation using CN as test case. Section 5 presents calculated excitation cross-sections for CN and section 6 gives our conclusions.

2. Method

The initial starting point of this theory is the work of Corey and McCourt (1983), whose work outlined the calculation of cross-sections for a collision between a $^{2S+1}\Sigma$ linear molecule and an atom in a ^{1}S state, using a Hund's case (b) coupling scheme. The general idea is that the electron spin is only weakly coupled to the molecular rotation and it plays a spectator role in the collision dynamics. In such a treatment, the dynamical problem is reduced to a spin-free problem where the energy splitting of the spin multiplets is neglected and the spin wave functions are decoupled from the rotational wave functions using a recoupling scheme. This 'recoupling' approach is adapted at collisional energies much larger than the energy splittings, which are typically below 1 meV for doublet and triplet targets. In order to implement collisions with electrons, the spin of the projectile needs to be incorporated into the coupling scheme of the existing work.

2.1. Coupling in case when the projectile is spinless

Using the general case of Corey and McCourt (1983), we adapt the angular momentum coupling scheme to include a spin-1/2 electron projectile. Using the definitions from Corey and McCourt (CM):

- **N** is the rotational angular momentum of molecule;
- **S** is the electron spin angular momentum of the molecule;
- **j** = **N** + **S** is the total angular momentum of the molecule;
- **l** is the orbital angular momentum of the projectile;
- **J** = **l** + **j** is total angular momentum of the compound system.

CM use a total-J basis represented by the coupling scheme, equation (CM2.10):

$$\mathbf{N} + \mathbf{l} = \mathcal{J}, \quad \mathcal{J} + \mathbf{S} = \mathbf{J}. \tag{1}$$

This basis is defined through equation (CM2.11)

$$|(Nl)\mathcal{J}S; JM\rangle = \sum_{m,m_S} (-1)^{-\mathcal{J}+S-M}[J]^{1/2} \times \begin{pmatrix} \mathcal{J} & S & J \\ \mathcal{M} & m_s & -M \end{pmatrix} |Nl\mathcal{J}\mathcal{M}\rangle\, |Sm_s\rangle\,, \tag{2}$$

where $|Nl\mathcal{J}\mathcal{M}\rangle$ is defined by equation (CM2.12)

$$|Nl\mathcal{J}\mathcal{M}\rangle = \sum_{m_N,m_l} (-1)^{-N+l-\mathcal{M}}[\mathcal{J}]^{1/2} \times \begin{pmatrix} N & l & \mathcal{J} \\ m_N & m_l & -\mathcal{M} \end{pmatrix} |Nm_N\rangle\, |lm_l\rangle\,, \tag{3}$$

where the $[x]$ is used to represent a factor of $(2x + 1)$.

Thus if one has T-matrices in the $|Nm_N\rangle\,|lm_l\rangle$ basis, they can be converted to the $|Nl\mathcal{J}\mathcal{M}\rangle$ basis using the above, subject to the condition $\mathcal{J}$ = **N** + **l**.

2.2. Case when the projectile has spin = 1/2

The above case of coupling can be adapted by redefining some variables and adding a new one to define the projectile electron spin. In this new coupling scheme the spin momenta and non-spin momenta are calculated in parallel before being combined in the final coupling stage:

- **N** is rotational angular momentum of molecule;
- $\mathbf{S}_m$ is electron spin angular momentum of the molecule;
- **s** is spin of projectile electron, **s** = 1/2;
- **S** is total spin angular momentum of the system, **S** = $\mathbf{S}_m$ + **s**;

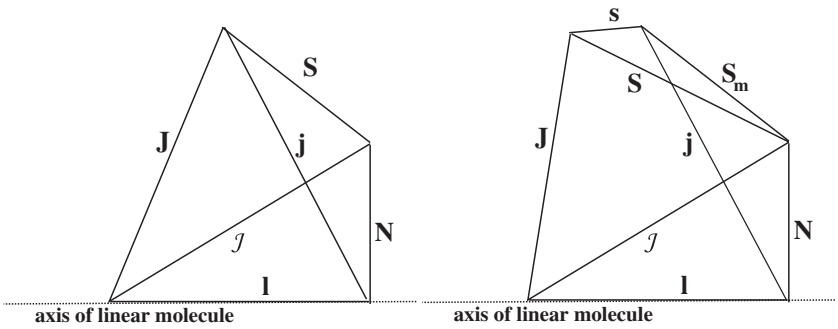

Figure 1. Comparison of the old (Corey and McCourt (1983), left) and new (right) coupling schemes.

- **j** defined as previously, $\mathbf{j} = \mathbf{N} + \mathbf{S}_m$;
- **l** is angular momentum of the projectile.

In this case we still use equation (1):

$$\mathbf{N} + \mathbf{l} = \mathcal{J}, \quad \mathcal{J} + \mathbf{S} = \mathbf{J}. \tag{4}$$

but with a generalized definition of **S**:

$$\mathbf{S} = \mathbf{S_m} + \mathbf{s} = S_m \pm 1/2. \tag{5}$$

Both schemes are shown in figure 1, note the difference in definition of molecular spin, **j** and **J** between the original (left) and the new (right) schemes. Figure 1 also provides the triangulation limits on the summations in equations (6)–(9) below.

Within our chosen coupling scheme, the spin and other angular momenta are coupled separately and then joined. Therefore the electron scattering T-matrices can be transformed by using equation (3), before including the extra weighted summation over S arising from the need to consider projectile spin. Adapting equation (CM2.27):

$$T^{JS}_{N'j'l',Njl} = \sum_{\mathcal{J}} (-1)^{j'-l'-j+l} [\mathcal{J}][j', j]^{1/2} \times \begin{Bmatrix} S & N & j \\ l & J & \mathcal{J} \end{Bmatrix} \begin{Bmatrix} S & N' & j' \\ l' & J & \mathcal{J} \end{Bmatrix} T^{\mathcal{J}S}_{N'l',Nl} \tag{6}$$

where the superscript S notation shows that the total electron spin is treated as a constant of motion for a given T-matrix.

2.3. Rotational cross-sections

Once the T-matrices have been transformed to the necessary basis, the scattering observables can be calculated using the following equations. Equation (CM2.28) gives the scattering amplitude from state $NSjm$ to state $N'Sj'm'$:

$$\begin{aligned} f(N'Sj'm' \leftarrow NSjm|\hat{R}) &= \left(\frac{\pi}{kk'}\right)^{1/2} \sum_{Jll'm_{l'}} i^{l-l'+1} [l]^{1/2} [J] \\ &\quad \times \begin{pmatrix} j & J & l \\ m & -m & 0 \end{pmatrix} \begin{pmatrix} j' & J & l' \\ m' & -m & m_{l'} \end{pmatrix} T^{JS}_{N'j'l',Njl} Y_{l'm_{l'}}(\hat{R}) \\ &= \left(\frac{\pi}{kk'}\right)^{1/2} \sum_{Jll'm_{l'}} \sum_{\mathcal{J}} i^{l-l'-1} (-1)^{j'-l'-j+l} [\mathcal{J}J][jj'l]^{1/2} \\ &\quad \times \begin{Bmatrix} S & N & j \\ l & J & \mathcal{J} \end{Bmatrix} \begin{Bmatrix} S & N' & j \\ l' & J & \mathcal{J} \end{Bmatrix} \begin{pmatrix} j & J & l \\ m & -m & 0 \end{pmatrix} \\ &\quad \times \begin{pmatrix} j' & J & l' \\ m' & -m & m_{l'} \end{pmatrix} T^{\mathcal{J}S}_{N'l',Nl} Y_{l'm_{l'}}(\hat{R}). \end{aligned} \tag{7}$$

The state-to-state differential cross-section is then given by equation (CM2.29):

$$\begin{aligned} \frac{\mathrm{d}\sigma}{\mathrm{d}\Omega}(N'Sj' \leftarrow NSj) &= (2j+1)^{-1} \frac{k'}{k} \sum_{m'm} |f(N'Sj'm' \leftarrow NSjm|\hat{R})|^2. \end{aligned} \tag{8}$$

Finally, the integral cross-section for a given S is given by equation (CM2.30):

$$\begin{aligned} \sigma^S(N'j' \leftarrow Nj) &= \frac{\pi}{(2j+1)k^2} \sum_{Jll'} [J] |T^{JS}_{N'j'l' \leftarrow Njl}|^2 \\ &= \frac{\pi}{k^2} \sum_{\mathcal{J}\mathcal{J}'} \sum_{Jll'} [J\mathcal{J}'\mathcal{J}j'] \begin{Bmatrix} S & N & j \\ l & J & \mathcal{J} \end{Bmatrix} \\ &\quad \times \begin{Bmatrix} S & N' & j' \\ l' & J & \mathcal{J} \end{Bmatrix} \begin{Bmatrix} S & N & j \\ l & J & \mathcal{J}' \end{Bmatrix} \\ &\quad \times \begin{Bmatrix} S & N' & j' \\ l' & J & \mathcal{J}' \end{Bmatrix} T^{\mathcal{J}S}_{N'l',Nl} T^{\mathcal{J}'S*}_{N'l',Nl}. \end{aligned} \tag{9}$$

However a weighted summation over S is required to obtain the observable cross-section

$$\sigma(N'j' \leftarrow Nj) = \sum_{S=|S_m-s|}^{S_m+s} \frac{(2S+1)}{n} \sigma^S(N'j' \leftarrow Nj) \tag{10}$$

with

$$n = \sum_{S=|S_m-s|}^{S_m+s} (2S+1). \tag{11}$$

This summation is not required in the original theory of Corey and McCourt (1983), as there is only a single value of S in their scheme.

3. The infinite order sudden approximation

Spin-coupled cross-sections may also be obtained through manipulation of the pure rotational cross-sections using the IOS approximation. This approximation is very similar to the adiabatic nuclei rotation (ANR) approximation in the electron–molecule literature (Lane 1980). This latter was employed in all previous R-matrix studies, combined with the Born or Coulomb–Born theory (see references in section 1). The ANR and IOS approximations consist of assuming that the target rotational states are degenerate, which is valid when the rotational spacings are negligible with respect to the collisional energy. Within such a treatment, the sum

of cross-sections over a final state is independent of the initial state. The IOS or ANR approximation was shown to be valid down to threshold in the case of the electron–H_3^+ system (Faure *et al* 2006), owing to the strong Coulomb field which ensures that the time scale for electron motion is always rapid compared to nuclear motion. In the case of a neutral target, the IOS approach is expected to fail at threshold, and a kinematic correction is usually employed (see below). Corey and McCourt (1983) have shown that within the IOS approximation, the spin-coupled or fine structure cross-sections can be directly obtained from the 'fundamental' pure rotational cross-sections, i.e. those out of the lowest $N = 0$ level. In practice, this is the method used below to calculate our data.

Rabadán *et al* (1998b) describe how to calculate rotational cross-sections using T-matrices produced by the R-matrix method (Tennyson 2010), employing the ANR approximation to allow the body-frame T-matrices to be transformed to the laboratory frame:

$$T^{\mathcal{J}S}_{N'l',Nl} \approx \sum_{\Lambda=-l}^{l} A^{\mathcal{J}\Lambda}_{N',l'} T^{\Lambda S}_{l',l} A^{\mathcal{J}\Lambda}_{N,l}, \tag{12}$$

where Λ is the projection of l over the nuclear axis and where

$$A^{\mathcal{J}\Lambda}_{N,l} = \sqrt{\frac{2N+1}{2\mathcal{J}+1}} C(Nl\mathcal{J}; 0\Lambda - \Lambda), \tag{13}$$

where $C(.)$ is a Clebsch–Gordan coefficient. From these, the integrated rotational cross-sections are then calculated using:

$$\sigma^{RM}(N' \leftarrow N) = \frac{\pi}{(2N+1)k_i^2} \sum_{\mathcal{J}=0}^{\infty} \sum_{l=|\mathcal{J}-N|}^{\mathcal{J}+N} \times \sum_{l'=|\mathcal{J}-N'|}^{\mathcal{J}+N'} (2\mathcal{J}+1) \left|T^{\mathcal{J}S}_{N'l',Nl}\right|^2, \tag{14}$$

where k_i is the initial momentum of the electron. In practice, the partial-wave expansion is truncated to some finite maximum value of l. This formulation has been implemented in the fortran program ROTLIN, written by Faure *et al* (2007). We have used the ROTLIN program to produce the pure rotational cross-sections for this work, subsequently calculating the spin-coupled data using the IOS approximation outlined in Corey and McCourt (1983).

Within the IOS approximation, the spin-coupled, degeneracy-averaged integrated cross-sections are given by equation (CM4.11):

$$\sigma^S(N'Sj' \leftarrow NSj) = \sum_{\lambda=0}^{N+N'} [N'Nj'] \begin{pmatrix} N' & N & \lambda \\ 0 & 0 & 0 \end{pmatrix}^2 \times \begin{Bmatrix} \lambda & j & j' \\ S_m & N' & N \end{Bmatrix}^2 \sigma^S(\lambda \leftarrow 0) \tag{15}$$

where $\sigma(\lambda \leftarrow 0)$ is defined explicitly by

$$\sigma^S(\lambda \leftarrow 0) \equiv \frac{\pi}{k_i^2} \sum_{l'l} \frac{[l'l]}{[\lambda]} \begin{pmatrix} l' & l & \lambda \\ 0 & 0 & 0 \end{pmatrix}^2 \left|T^{lS}_{\lambda}\right|^2. \tag{16}$$

This is equivalent to the pure rotational cross-section out of the lowest $N = 0$ level, for a given S

$$\sigma^S(\lambda \leftarrow 0) \equiv \sigma^S(N' \leftarrow 0). \tag{17}$$

The total cross-section is then obtained using equation (10).

Using this method we have generalized on the code ROTLIN to the create ROTLIN_S which implements this IOS approximation method to add the spin-coupling to the pure rotational cross-sections. This is done by specifying the required values of j and j' as user input, where they can take the values

$$|N - S_m| \leqslant j \leqslant N + S_m \tag{18}$$

and

$$|N' - S_m| \leqslant j' \leqslant N' + S_m \tag{19}$$

in integer steps of j, j'.

The original ROTLIN code also implemented a Born correction for $\Delta N = 1$ transitions, this is especially important when the dipole moment of the molecule is large (say $\gtrsim 1$ D) and the Born cross-section becomes dominant (Faure *et al* 2004). In this case, the standard procedure is to use the dipolar Born approximation to obtain the cross-section for the high partial waves not included in the body-frame T-matrices (Norcross and Padial 1982). The resulting $\Delta N = 1$ spin-rotation cross-sections produced also incorporate the Born correction correctly.

Finally, as mentioned above, the expected unphysical behaviour of the IOS cross-sections near rotational thresholds was corrected using a simple kinematic ratio (Chang and Temkin 1969, Rabadán *et al* 1998b) which forces the excitation cross-sections to zero at the rotational threshold:

$$\sigma^{\text{final}}(N'j' \leftarrow Nj) = \frac{k_f}{k_i} \sigma(N'j' \leftarrow Nj), \tag{20}$$

where k_f is the final momentum of the electron, which is equal to zero at threshold. The exact threshold law is however not known. We note that threshold as well as closed-channel effects can only be included rigorously in full close-coupling calculations (Faure *et al* 2006).

4. Testing the IOS approximation

Corey and McCourt (1983) showed that a consequence of the IOS approximation is that cross-sections for any transition $N' \leftarrow N$ can be deduced from the fundamental rotational cross-sections $\sigma(\lambda \leftarrow 0)$. Namely equation (CM5.8),

$$\sigma(N' \leftarrow N) = \sum_{\lambda=0}^{N+N'} [N'] \begin{pmatrix} N' & N & \lambda \\ 0 & 0 & 0 \end{pmatrix}^2 \sigma(\lambda \leftarrow 0) \tag{21}$$

where $\sigma(\lambda \leftarrow 0)$ are the pure rotational cross-sections out of the $N = 0$ level. This property can thus be tested in the present context. Indeed, in the above treatment the IOS approximation was combined with both a Born and a threshold correction and the rotational spacings were thus taken into account in the final cross-sections. Also the above sum over lambda is limited by the maximum of N and N' but is truncated in practice. Hence the above IOS property, equation (21), should not be fulfilled. However, if in practice the departure from equation (21) is small, as expected at high collision energy, the above IOS treatment for spin-coupled cross-sections should be reliable.

Recently Harrison and Tennyson (2012) published electron-collision data on the molecular radical CN using

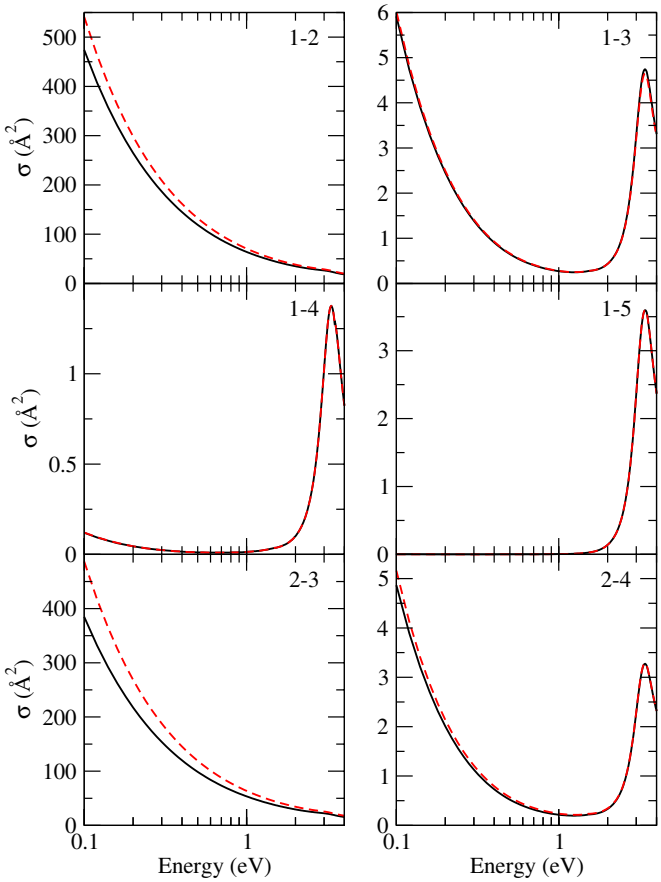

Figure 2. Electron-impact rotational excitation of CN ($N \rightarrow N'$) calculated using the full theory (solid) and the IOS approximation, equation 21 (dashed).

the *R*-matrix method. The *T*-matrices produced during these calculations are used here to calculate spin-rotational cross-sections from 0.1 to 4 eV. We use this example to test whether the IOS approximation holds, and also to produce some initial spin-rotational cross-sections for CN (see next section). Figure 2 presents comparisons of the directly calculated $\sigma(N' \leftarrow N)$ pure rotational cross-sections, which include the Born and threshold corrections, with those calculated using the IOS equation (21) above for a number of transitions.

Clearly there is excellent correlation between the two calculations for all transitions. The slight discrepancies at low energy (lower than $\sim 25\%$) can be explained because (i) the target rotational levels are not treated as degenerate in the Born regime and (ii) the rotational thresholds are included in the full calculation through the kinematic ratio, equation (20). However there is in general an excellent correlation between the two calculations, demonstrating that equation (21) and by extension equation (15) is reliable. We therefore conclude that the IOS approximation is applicable in the energy regime investigated and can be used to simplifying the full spin-coupling theory. We note that at lower energy, it is possible to improve the IOS approach by scaling the IOS spin-recoupled cross-sections by the pure rotational cross-sections, as done by Faure *et al* (2007) for the hyperfine rate coefficients of HCN. Full details about this scaling procedure, which becomes necessary for collision energies below 0.1 eV owing to the failure of the IOS assumption, will be discussed elsewhere.

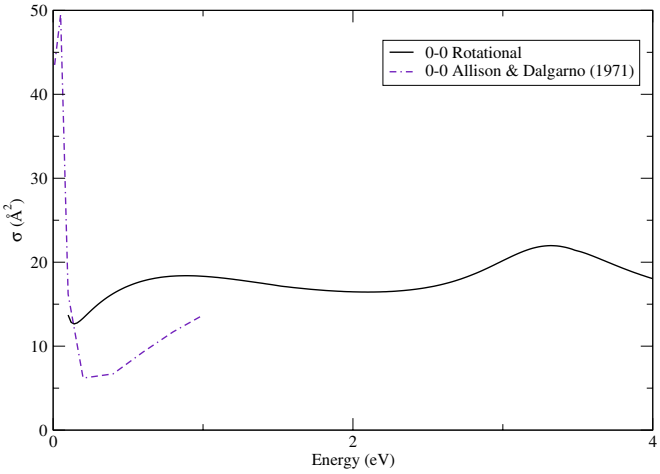

Figure 3. CN $N = 0$–0 elastic rotationally-resolved cross-section.

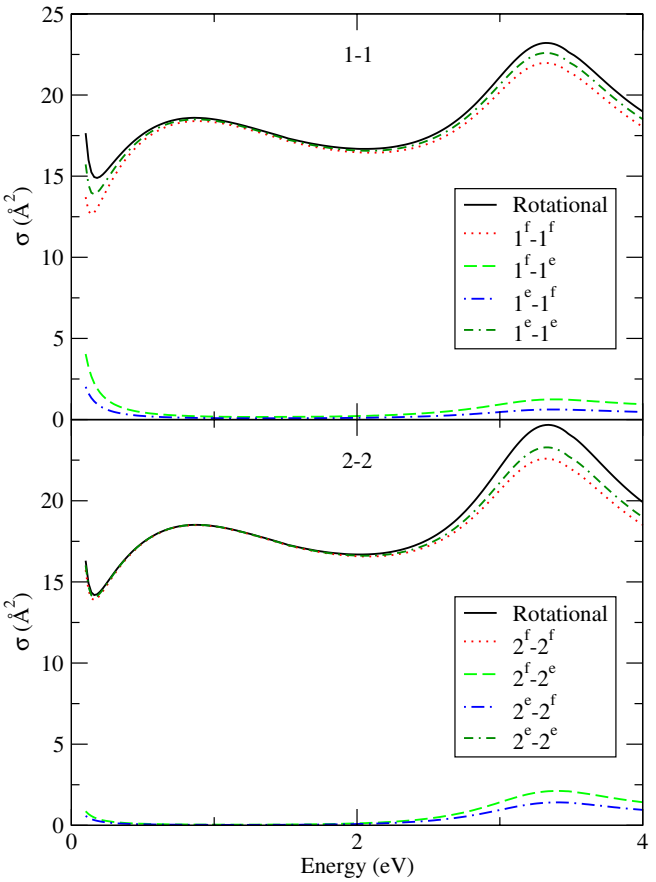

Figure 4. CN $N = 1$–1 and $N = 2$–2 spin-rotational resolved elastic cross-sections.

5. Sample results: cross-sections for CN

The CN *T*-matrices have also been used to produce some example results. Details of the original *R*-matrix calculations which produced these *T*-matrices can be found in Harrison and Tennyson (2012). In running these calculations a rotational constant of 1.899 cm^{-1} and the experimental dipole moment

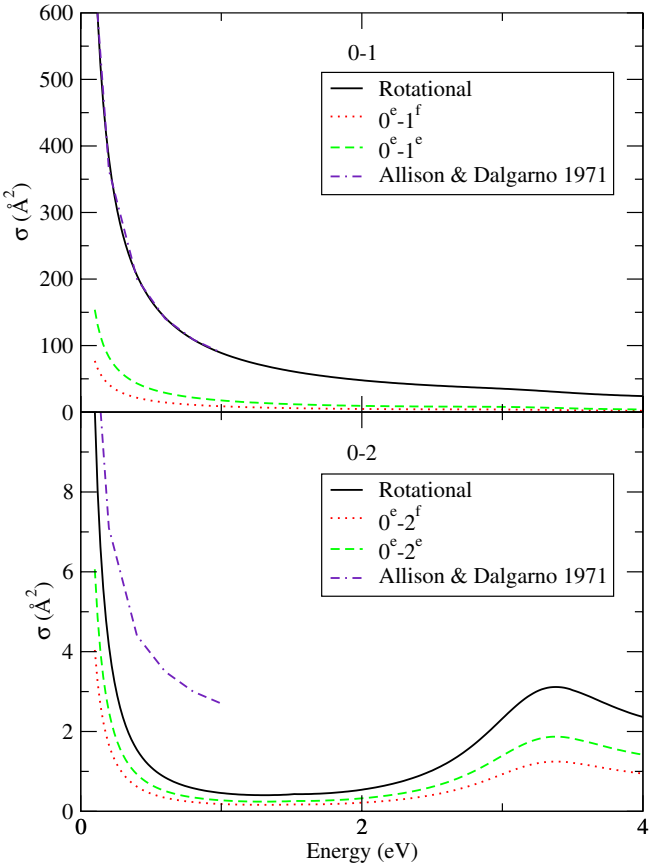

Figure 5. CN $N = 0$–1 and $N = 0$–2 spin-rotational excitation cross-sections.

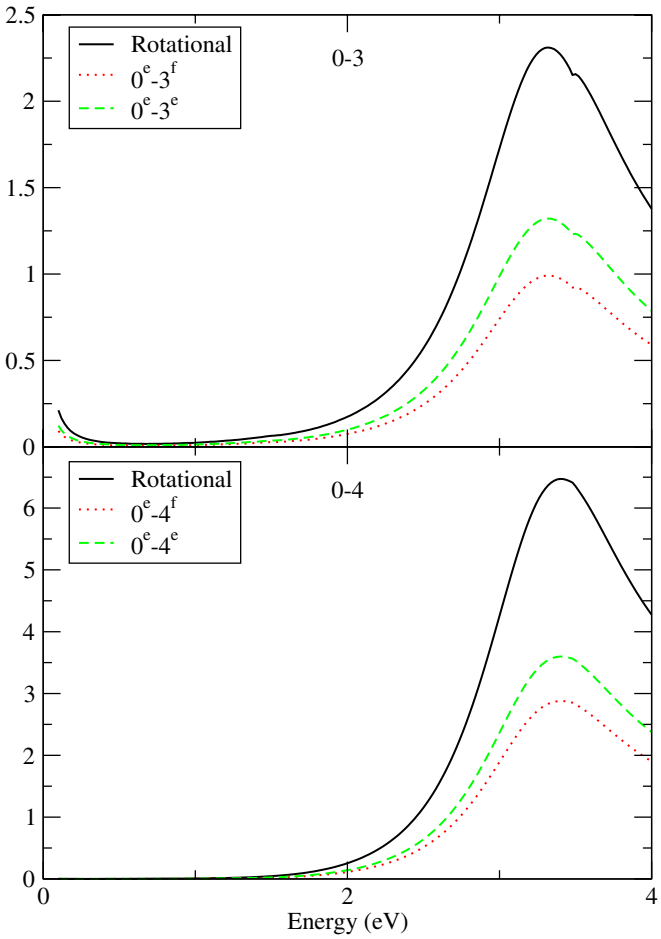

Figure 6. CN $N = 0$–3 and $N = 0$–4 spin-rotational excitation cross-sections.

of 1.45 D (Thompson and Dalby 1968) were used in the outer region.

Each rotational level of CN is split by spin-rotation coupling so that rotational level N has two sub-levels given by $j = N \pm 1/2$; conventionally each of these are labelled using N and the e or f label for the splitting (Brown *et al* 1975). Levels with parity $+(-1)^{j-1/2}$ are e levels ($j = N+1/2$), while levels with parity $-(-1)^{j-1/2}$ are f levels ($j = N - 1/2$). Radiative (dipolar) selection rules are:

$$\Delta j = 0, e \leftrightarrow f, \qquad \Delta j = \pm 1, e \leftrightarrow e \text{ and } f \leftrightarrow f. \tag{22}$$

Figures 3–7 present both the pure rotational (rotational) and spin-rotational cross-sections for the $0 \rightarrow N$ ($N = 0, 1, 2, 3, 4$), $1 \rightarrow 1$, $2 \rightarrow 2$, $1 \rightarrow 2$ and $1 \rightarrow 3$ transitions, for incident electron energies up to 4 eV. The e/f notation in the legends indicating the spin-resolved transition between states as discussed in the previous paragraph. It is important to note that above the A $^2\Pi$ excitation threshold at 1.515 eV, electronic excitations are also possible. However, what is clearly visible in the figures is the resonance feature associated with the B $^2\Sigma^+$ excitation at 3.49 eV. The resonance region is the energy range where transitions with $\Delta N > 2$ are significant but, conversely, it does not significantly affect the dipole-dominated $\Delta N = 1$ transitions. We also note the 0–0 elastic rotational cross-section is not changed by introducing spin-coupling, as both j and j' may only have the value $1/2$. Cross-sections up to and included $\Delta N = 6$ were calculated and considered, however those beyond $\Delta N = 4$ are all very small, below 0.01 Å^2 and are not considered here.

In figure 3, the present pure elastic 0–0 cross-section is compared to the old close-coupling calculations of Allison and Dalgarno (1971). Both calculations are found to agree at the lowest energy (0.1 eV) while at higher energy, our value is much larger, reflecting most probably the much better treatment of the short-range forces as well as the possible role of the above mentioned resonances.

Very similar elastic cross-sections are obtained for levels $N = 1$ and 2, as plotted in figure 4. We also observe for these 'quasi-elastic' transitions ($\Delta N = 0$) that parity-changing transitions ($e \leftrightarrow f$) have much lower cross-sections than parity-conserving transitions. This propensity rule is further discussed below.

In figure 5, the 0–1 and 0–2 rotational cross-sections are compared to the results of Allison and Dalgarno (1971). The large dipolar 0–1 cross-sections are found in excellent agreement, as expected since the dipole moment used is the same in both calculations. The present 0–2 cross-section is found to be significantly lower than that of Allison and Dalgarno (1971), as this transitions is dominated by short-range effects, this again shows the importance of the R-matrix treatment. It is also about two orders of magnitude lower than the 0–1 cross-section. We also observe that the largest

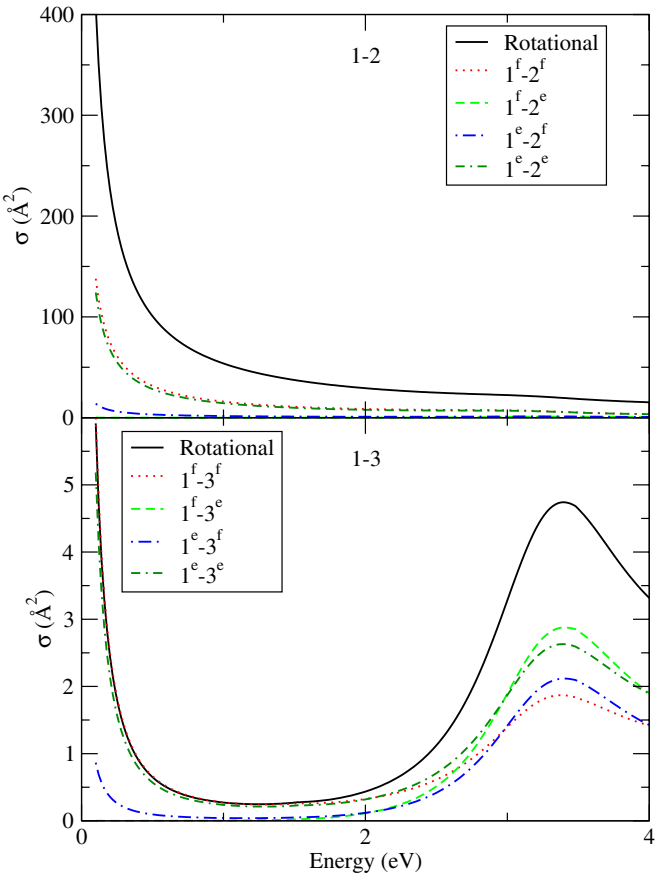

Figure 7. CN $N = 1$–2 and $N = 1$–3 spin-rotational cross-sections.

spin-rotational cross-sections are those corresponding to parity-conserving transitions. This propensity rule, which can be written $\Delta j = \Delta N$, is a general feature of any molecule in $^{2S+1}\Sigma$ electronic state as described theoretically in Alexander *et al* (1986). For $\Delta j = 1$ it thus follows the above radiative selection rule. At the IOS level, it can be explained simply from the $3j$ and $6j$ coefficients in equation (15). We note that this propensity rule is also observed in the recent close-coupling calculations of Lique and Klos (2011) and Kalugina *et al* (2012) on CN–He and CN–H_2, respectively.

Figure 6 shows that 0–3 and 0–4 cross-sections are much lower than the 0–2 cross-section, except in the region of the B $^2\Sigma^+$ resonance where the 0–4 cross-section, in particular, is significantly amplified and becomes larger than the 0–2 cross-section. This is expected to have important consequences on the spin-coupled cross-sections, as discussed below. Again we observe that parity-conserving transitions ($\Delta j = \Delta N$) are preferred.

Finally, figure 7 gives cross-sections for $\Delta N = 1, 2$ transitions out of the $N = 1$ parity doublet. The dipolar 1–2 rotational cross-section is found to be comparable to the 0–1 cross-section and the propensity rule $e \leftrightarrow e, f \leftrightarrow f$ is clearly in evidence for all transitions at collision energy below about 2 eV. However, at higher energy, the parity-changing transition $1^f - 3^e$ is surprisingly found to become dominant. This illustrates the strong impact of the resonance associated with the B $^2\Sigma^+$ excitation at 3.49 eV. Indeed, this resonance greatly enhances the 0–3 and 0–4 cross-sections (see figure 6) which, in turn, increase $\Delta j = 3$ cross-sections through equation (15).

6. Conclusions

In this paper we have presented a new theory of calculating spin-coupled rotational cross-sections for electron collisions with neutral linear molecules in a $^{2S+1}\Sigma^+$ ground state. This is based on the initial work of Corey and McCourt (1983), who outlined the details of a ^{1}S atom colliding with a linear molecule in a $^{2S+1}\Sigma^+$ ground state. This work has already provided the equations required for calculating the state to state differential, and integrated cross-sections from the collision T-matrices of the appropriate basis. By introducing projectile spin to represent the colliding electron, and coupling this to the target molecule spin, we have presented an altered coupling scheme which can still be used in the existing theoretical framework.

However, by applying the IOS approximation, we are able to greatly simplify the theory to obtain the spin-coupled cross-sections by simple manipulation of the pure rotational data. The viability of using this approximation has been tested using existing input T-matrices from electron–CN scattering calculations (Harrison and Tennyson 2012), and found to be applicable in this scheme. The use of IOS approximation has also enabled a successful integration into the existing ROTLIN fortran program, which calculates pure rotational cross-section using the T-matrix output from an electron–molecule scattering calculation using the R-matrix method (Tennyson 2010). This has led to the development of the new ROTLIN_S program, which enables the spin-coupled cross-sections to be calculated with the addition of new user input which will be implemented as a module within the UK molecular R-matrix code (Carr *et al* 2012). Example data has been presented for the $(0 \rightarrow N)$, $(N = 0$–$4)$, $1 \rightarrow 2$ and $1 \rightarrow 3$ rotational cross-sections for an electron–CN collision. These results are heavily influenced by both the A $^2\Pi$ and B $^2\Sigma^+$ excitation thresholds at 1.52 and 3.49 eV respectively. The latter in particular leading to an enhancement of the cross-sections. At energy below these electronic thresholds, the usual propensity rule for parity-conserving transitions ($\Delta j = \Delta N$) was found to hold.

Further work planned is to extend the database of electron–CN rotational cross-sections up to higher N values and hence to provide a full suite of cross-sections and associated rates to the astronomical community. These results will be published elsewhere.

Acknowledgment

The first author would like to thank the STFC for a studentship. François Lique is thanked for useful discussions.

References

Ahearn M F, Millis R L, Schleicher D G, Osip D J and Birch P V 1995 *Icarus* **118** 223–70

Alexander M H, Smedley J E and Corey G C 1986 *J. Chem. Phys.* **84** 3049–58

Allison A C and Dalgarno A 1971 *Astron. Astrophys.* **13** 331–2

Brown J M, Hougen J T, Huber K P, Johns J W C, Kopp I, Lefebvre-Brion H, Merer A J, Ramsay D A, Rostas J and Zare R N 1975 *J. Mol. Spectrosc.* **55** 500–3
Bus S J, Ahearn M F, Schleicher D G and Bowell E 1991 *Science* **251** 774–7
Carr J M, Galiatsatos P G, Gorfinkiel J D, Harvey A G, Lysaght M A, Madden D, Masin Z, Plummer M and Tennyson J 2012 *Eur. J. Phys.* D **66** 58
Chang E S and Temkin A 1969 *Phys. Rev. Lett.* **23** 399
Chu S I and Dalgarno A 1974 *Phys. Rev.* A **10** 788–92
Corey G C and McCourt F R 1983 *J. Phys. Chem.* **87** 2723–30
Crawford O H, Allison A C and Dalgarno A 1969 *Astron. Astrophys.* **2** 451
Dubernet M L *et al* 2012 *Astron. Astrophys.* submitted
Faure A, Gorfinkiel J D and Tennyson J 2004 *J. Phys. B: At. Mol. Opt. Phys.* **37** 801–7
Faure A, Kokoouline V, Greene C H and Tennyson J 2006 *J. Phys. B: At. Mol. Opt. Phys.* **39** 4261–73
Faure A and Tennyson J 2001 *Mon. Not. R. Astron. Soc.* **325** 443–8
Faure A and Tennyson J 2002a *J. Phys. B: At. Mol. Opt. Phys.* **35** 3945–56
Faure A and Tennyson J 2002b *J. Phys.B: At. Mol. Opt. Phys.* **35** 1865–73
Faure A, Varambhia H N, Stoecklin T and Tennyson J 2007 *Mon. Not. R. Astron. Soc.* **382** 840–8
Fray N, Benilan Y, Cottin H, Gazeau M C and Crovisier J 2005 *Planet. Space Sci.* **53** 1243–62
Giannetti A, Brand J, Massi F, Tieftrunk A and Beltran M T 2012 *Astron. Astrophys.* **538** A41
Harrison S and Tennyson J 2012 *J. Phys. B: At. Mol. Opt. Phys.* **45** 035204
Itikawa Y and Mason N 2005 *J. Phys. Chem. Ref. Data* **34** 1–22
Jimenez-Serra I, Martin-Pintado J, Viti S, Martin S, Rodriguez-Franco A, Faure A and Tennyson J 2006 *Astrophys. J.* **650** L135–8
Kalugina Y, Lique F and Kos J 2012 *Mon. Not. R. Astron. Soc.* **422** 812–8
Lane N F 1980 *Rev. Mod. Phys.* **52** 29–119
Leach S 2012 *Mon. Not. R. Astron. Soc.* **421** 1325
Lim A J, Rabadán I and Tennyson J 1999 *Mon. Not. R. Astron. Soc.* **306** 473–8
Lique F and Klos J 2011 *Mon. Not. R. Astron. Soc.* **413** L20–3
Lopez-Duran D, Bodo E and Gianturco F 2008 *Comput. Phys. Commun.* **179** 821–38
Norcross D W and Padial N T 1982 *Phys. Rev.* A **25** 226–338
Rabadán I, Sarpal B K and Tennyson J 1998a *Mon. Not. R. Astron. Soc.* **299** 171–5
Rabadán I, Sarpal B K and Tennyson J 1998b *J. Phys. B: At. Mol. Opt. Phys.* **31** 2077–90
Rabadán I and Tennyson J 1998 *Comput. Phys. Commun.* **114** 129–41
Roberts J F, Jimenez-Serra I, Martin-Pintado J, Viti S, Rodriguez-Franco A, Faure A and Tennyson J 2010 *Astron. Astrophys.* **513** A46
Roth K C, Meyer D M and Hawkins I 1993 *Astrophys. J.* **413** L67–71
Shafir D *et al* 2009 *Phys. Rev. Lett.* **102** 223202
Tennyson J 2010 *Phys. Rep.* **491** 29–76
Thompson R and Dalby F W 1968 *Can. J. Phys.* **46** 2815–9
Varambhia H N, Faure A, Graupner K, Field T A and Tennyson J 2010 *Mon. Not. R. Astron. Soc.* **403** 1409–12
Varambhia H N, Gupta M, Faure A, Baluja K L and Tennyson J 2009 *J. Phys. B: At. Mol. Opt. Phys.* **42** 095204
Zhang R, Faure A and Tennyson J 2009 *Phys. Scr.* **80** 015301